COBEM 2023 27TH INTERNATIONAL CONGRESS OF MECHANICAL ENGENEERING

ABCM Brazilian Society of Mechanical Sciences and Engineering
27th ABCM International Congress of Mechanical Engineering
December 04-08, 2023, Florianópolis-SC, Brazil

COB-2023-0210
ANALISYS OF THE RAREFIED FLOW IN MICROCHANNEL WITH VARIOUS GEOMETRIES

Vinícius Daher[(1,2)]
Ruan Ramon Passos Penha Pereira[(2)]
Cayo Prado Fernandes Francisco[(2)]
(1) Instituto Tecnológico de Aeronáutica – ITA, Pç Mal. Eduardo Gomes 50, São José dos Campos, SP, 12228-900, Brazil
(2) Instituto de Aeronáutica e Espaço – IAE, Pç Mal. Eduardo Gomes 50, São José dos Campos, SP, 12228-904, Brazil
vinicius_daher@hotmail.com,passos.ruan@gmail.com, cayo.francisco@gmail.com.

Abstract. *The use of microelectromechanical systems (MEMS) offer great potential to meet technological requirements in miniaturized systems. For example, implementing MEMS-scale space thrusters, as well as microfluidic machines, such as micropumps and microcompressors present new challenges in manufacturing, material compatibility, and fluid dynamics modeling. Understanding flow behavior at micro and nanoscales, where the continuum hypothesis is not always applicable, is essential for the development of more efficient MEMS designs. In this paper, a Poiseuille-type flow of a rarefied gas through microchannels with three different geometries and isothermal wall conditions was investigated numerically. The simulations were performed using the Direct Numerical Simulation Monte Carlo(DSMC) technique for 3 degrees of rarefaction, with Knuden numbers (Kn) 0,027, 0,055 and 0,11 corresponding to the transitional regime, along a straight microchannel, a microchannel with 90 degrees curvature and a rounded 90 degree bend. The results obtained indicated that the inclusion of a curvature in the microchannel had a positive impact on the amount of mass transport. Also, the rounding on the curvature of the microchannel allowed an additional efficiency gain in relation to the pressure drop magnitude.*

Keywords: *DSMC, microflow, microchannel, rarefied flow.*

1. INTRODUCTION

Rarefied flows are typically associated with problems involving the aerodynamics of spacecraft in low Earth orbits or undergoing atmospheric reentry maneuvers. However, rarefied flow, where the assumption of linear constitutive relations in the Navier-Stokes-Fourier (NSF) equations is no longer applicable, is also encountered in ambient conditions when the flow of gasses occur in reduced dimensions compared to the mean free path of the gas molecules.

This flow dynamics occurs, for example, in micro and nanodevices, which can be used in compact heat exchangers, electronic refrigeration applications, and internal combustion engines, among others. Also, pressure sensors for catheters in biomedical applications have extremely small dimensions, while microactuators move electron scanning microscopes to scan atoms, and surface micromachining devices on silicon have been successfully applied in microfabrication processes. Additionally, we have fluid flows in microchannels that can be applied in drag reduction technologies and turbulence control in aerospace vehicles, significantly impacting fuel economy, while microfluidic device networks are being researched for controlled drug delivery (Sharp et al., 2002; Gad-el-Hak ,1999), showcasing the wealth of applications for these technologies.

Currently, efforts are also underway to develop mechanisms known as "lab-on-a-chip" for the identification, separation, and purification of cells, biomolecules, toxins, nanoparticles, and other materials, leading, naturally, to the necessity to better understand the fluid mechanics at the micro and nanoscales to enable the development of such devices (Sharp et al., 2002; Gad-el-Hak ,1999), as quantifying diffusive heat and momentum transfer processes becomes essential for the efficient design of these devices, inherently driving the development of fundamental science and microdevice engineering.

Most studies in the field of computational simulation of microflows employ the well-known "Computational Fluid Dynamics" (CFD) technique to investigate a wide range of phenomena. However, within some problems, such as the one proposed in this work, local non-equilibrium effects can arise due to the reduced dimensions of the objects under study, leading to inaccurate simulation results. Furthermore, under these rarefied conditions, as highlighted above, the continuum hypothesis becomes weak and the application of CFD modeling becomes questionable. In recent years, new algorithms and theoretical models by Le et. al, (2007), Sebastião and Santos,(2014) e Jien Xie et al., (2019) have been developed to simulate with higher accuracy the collision processes between fluid molecules and the interaction between these molecules and solid surfaces at micro and nano scales. This makes the Direct Simulation Monte Carlo (DSMC) method the most suitable tool for computational analysis and modeling of flows in this regime.

2. OBJECTIVE

The objective of this study is to analyze the behavior of rarefied flows induced by pressure gradients in microchannels with varied geometries. Specifically, the goal is to analyze parameters such as mass flow rate, heat flux, and momentum flux under the aforementioned physical conditions using computational simulations involving the DSMC technique (Bird, 1994; Cercignani, 2000).

3. PHYSICAL PROBLEM

The flow of gases is classified as rarefied when the mean free path between gas molecules is comparable to or greater than the characteristic length of the flow. In these cases, macroscopic properties of the flow, such as density and temperature, can exhibit significant variations over small distances and classical models based on Navier-Stokes equations may not be physically accurate to describe the phenomena occurring in his regime.

The representation of gas flows in microgeometries can deviate from the conventional theory established by the continuity hypothesis of Classical Fluid Mechanics. The continuity premise neglects the microscopic discontinuities present in flows. Therefore, all macroscopic characteristics such as density, temperature, pressure, and velocity are considered continuous from point to point. This is achieved by averaging microscopic properties over a sufficiently large sampling volume, encompassing a significant number of molecules, to avoid the influence of microscopic fluctuations. If the sampling volume is excessively small, fluctuations in the average value of a feature over the sampling volume occur due to variations in the number and type of molecules present inside it. At the same time, this sampling volume must be small enough for the local value of a macroscopic characteristic to be determined independently of spatial variations.

Rarefied flows naturally occur in microchannels and microfluidic devices, where the channel dimensions are of the order of micrometers or smaller. At these scales, gas rarefaction is often dominant, and the effects of molecular collisions become essential to understand and model flow behavior. The continuity premise also requires the presence of thermodynamic equilibrium within the sampling volume (local equilibrium). This implies that local thermodynamic properties in the sampling volume satisfy the same thermodynamic relationships as those of a system in equilibrium, even if this condition does not apply to the system as a whole. This assumption requires that the characteristic time associated with transient macroscopic processes (non-equilibrium processes) is considerably longer than the time required for the sampling volume to reach a suitable equilibrium state when isolated from the real system. Therefore, the frequency of intermolecular collisions within the sampling volume must be sufficiently high, implying that the mean free path of gas molecules, λ, the average distance traveled by a molecule between consecutive collisions, must be small compared to the size of the sampling volume. The ratio of the mean free path of molecules to a characteristic length of a geometry is called the Knudsen number.

The Knudsen number (Kn) is a dimensionless measure of the relative rarefaction of the gas, and its value is often used to distinguish between continuous and rarefied regimes. Due to the limitations of classical models based on the Navier-Stokes equations in describing rarefied flows in microchannels, it is necessary to resort to simulation methods that take into account the discrete nature of gas molecules.

In internal flows, such as those observed in microsystems, when the Knudsen number is not low, the effects of local thermodynamic non-equilibrium become relevant for the flow. This imbalance occurs in a fluid layer near the walls, called the Knudsen layer, where intermolecular interactions are less frequent compared to the core of the flow. The Knudsen layer extends away from the walls by an extent on the order of the mean free path. For smaller Knudsen numbers, this layer represents a very small portion of the domain. However, as Kn increases, this layer grows and increasingly influences the flow until the non-equilibrium condition encompasses the entire channel. Under these circumstances, the continuous assumption is no longer appropriate, and a molecular description becomes necessary. Similarly, the mean free time, which is the average time interval between consecutive collisions, must remain significantly shorter than the characteristic time associated with variations in macroscopic flow properties to ensure local equilibrium.

The Boltzmann equation serves as the foundation for the molecular description of flows. A crucial assumption in deriving this equation is the dilute gas hypothesis. In a dilute gas, most intermolecular collisions occur in a binary fashion, considerably simplifying the treatment of the collision term in the Boltzmann equation.

The study of rarefied flow in microchannels is a rapidly evolving research topic. With the increasing miniaturization of MEMS (Micro-Electro-Mechanical Systems) devices and the need to understand flow behavior in smaller-scale systems, microchannel flow has become a subject of great interest. In this regime, rarefied flow exhibits different behaviors compared to continuous flow, and the dynamics of transport properties are strongly influenced by the Knudsen number. A widely used method for simulating rarefied flows in microchannels is the DSMC (Direct Simulation Monte Carlo) method, which allows for simulations in different Knudsen number regimes.

Numerical research efforts focused on understanding rarefied flow in microchannels are crucial for the design and optimization of MEMS devices with improved performance and lower cost, as experimental studies at these scales are scarce and challenging to conduct. MEMS devices are designed to be compact, lightweight, and cost-effective, and their performance can be highly influenced by flow behavior in microchannels, as many MEMS devices are used in applications involving fluid flow, such as pumps and valves, while others may require heat exchange and the development

of enhanced microscale cooling devices to advance new technologies. Another ongoing research aspect is the development and testing of DSMC techniques that enable more accurate and efficient simulations of rarefied flows in microchannels, as simulations dealing with subsonic Mach numbers (Ma) are known to exhibit a significant amount of statistical scattering in flow properties due to low signal-to-noise ratio (Bird, 1994).

4. METHODOLOGY

The DSMC method was developed by Bird, (1994) and has become one of the most important methods for solving rarefied gas flows in the transitional regime. However, the DSMC method is not directly derived from the Boltzmann equation (Cercignani, 2000), but rather obtained from classical kinetic theory of rarefied gases. However, it has been shown recently that the DSMC method asymptotically converges to solutions of the Boltzmann equation, subject to the same assumptions as the Boltzmann equation, namely, molecular chaos and dilute gas hypotheses. The DSMC method instructs particles to move and collide using considerations from kinetic theory and accurately captures the behavior of the gas in non-equilibrium thermodynamic state. In the ballistic phase, molecules with velocities v_i travel, without interacting with each other, a distance Δx_i in a time interval Δt. The new positions are calculated from the previous positions using the following equation:

$$r_{i,n} = r_{i,a} + v_i \Delta t \qquad [4.1]$$

Intermolecular collisions, in turn, are calculated using stochastic procedures, where each computational particle represents a large number of actual gas molecules. The decoupling of the ballistic motion of the particles and the collision process significantly improves the computational efficiency of DSMC compared to other particle methods as shown by Bird (1994) and Cercignani (2000). Intermolecular collisions are performed in computational cells, where each cell has a size of a small fraction of the local mean free path (λ), and is used to probabilistically select the simulated particles for the collision process. Intermolecular collisions are modeled to reproduce the real behavior of the fluid when the flow is examined at a macroscopic level. For the rigid sphere model, the acceptance-rejection criterion, proposed by Bird, (1994), is applied using the following test:

$$\frac{v_r'}{(v_r')_{max}} > R_f \qquad [4.2]$$

Where v_r' is the maximum relative velocity of the particles in the computational cell and R_f is a randomly distributed number between 0 and 1. Subsequently, the macroscopic properties of the flow are sampled from the particle properties.

The DSMC code to be used in this project is the open-source code dsmcFoamPlus. The dsmcFoamPlus can be freely accessed through the OpenFOAM platform (OpenFOAM, 2019). For the intermolecular collision process, several models are implemented and the phenomenological Larsen-Borgnakke model is used for the redistribution of post-collision energy among the translational and rotational modes of the particles (Scanlon et al, 2010), while the QK model (Scanlon et al, 2010) is used to model the transfer of vibrational energy in highly energetic collisions.

In summary, the algorithm employed in the DSMC calculations can be sequentially represented as shown in the diagram below:

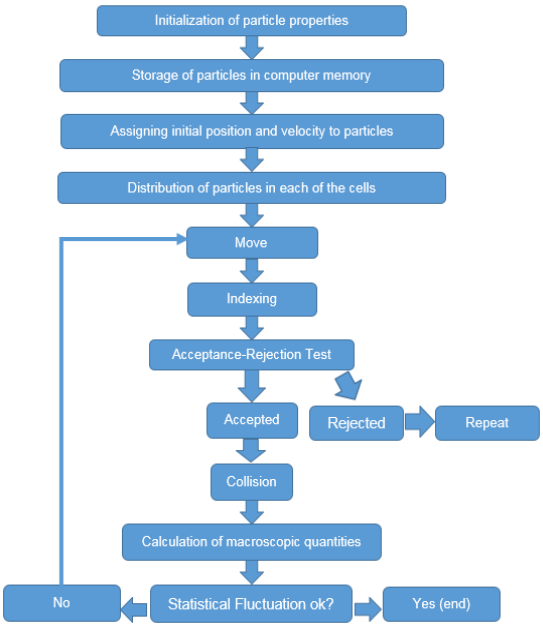

Figure 1. Flowchart of the DSMC Code.

The numerical analysis of a subsonic flow in a microchannel arising from a pressure difference requires a special approach to deal with the boundary conditions at the inlet and outlet. At the inlet, only two of the three flow parameters (pressure, temperature and velocity) can be freely specified, while at the outlet only one can be determined. However, in the DSMC method, all three flow parameters must be specified for molecules entering the domain boundaries, i.e., density, temperature, and velocity. Therefore, the boundary conditions need to be formulated based on the flow properties within the domain.

The application of the DSMC method to flow simulations that require implicit treatment of subsonic boundary conditions is more recent. Nance et al.,(1998) applied particle conservation in each cell to determine the unknown velocity at the exit. Fang & Liou,(2002) developed and tested a simpler approach, in which the unknown velocity at the input was estimated by extrapolation from the cell adjacent to the boundary.

The boundary conditions proposed by Wang & Li,(2004) propose that at the input boundary, the properties of the target gas are specified, that is, pressure and temperature, and the input numerical density is calculated based on the application of the perfect gas law. These velocities are obtained through first-order extrapolations from the properties of the cells connected to the respective boundary faces. At the exit of the microchannel, the only known flow property is pressure. Therefore, to determine the temperature and velocity, it is necessary to resort to the information available in the internal flow domain. The process of determining the necessary energies in terms of translation and rotation for particles located at the boundaries follows the practices established in the DSMC method. Detailed information can be found at Bird, (1994).

4.1 **Verification and Validation**

A fundamental step prior to conducting the simulations proposed here is the implementation of verification and validation processes of the dsmcFoamPlus code. The verification step, for the conditions studied, was performed considering a subsonic flow through a microchannel composed of two parallel plates. Due to the caracteristics of the OpenFOAM, a three-dimensional domain with only one mesh element for the width of the channel was generated in order to simulate a two-dimensional flow.

The code validation study was initiated by simulating rarefied flow in a straight microchannel with dimensions of 2μm x 0.4μm (length L and height H). The results were compared to those available in the literature by Sebastião and Santos, (2014); Le et al.,(2007); Liou and Fang, (2001) and Sebastião and Santos, (2013). Below, in Figure 2, a representative case of the microchannel flow is presented. The flow of nitrogen gas (N2) subjected to a pressure gradient between the ends of the microchannel was simulated. The inlet pressure was 252 kPa, and the outlet pressure was 100 kPa. The temperature of the walls, as well as that of the flow, was set to 300 K.

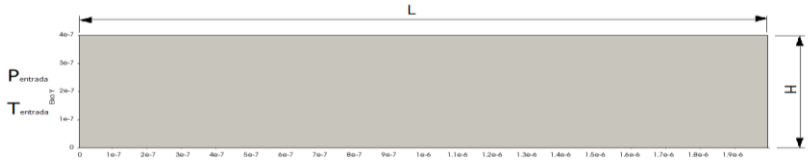

Figure 2 – Schematic representation of the initial condition of the verification case.

At the wall, diffusive boundary conditions were applied. For the computational domain each DSMC particle represents an equivalent number of real particles given by the "n equivalent" value,

$$n_{equivalent} = \left(\frac{P.V_{1cell}}{N_{particles\ per\ cell}}\right)_{in} = \left(\frac{P.V_{1cell}}{N_{particles\ per\ cell}}\right)_{out} \qquad [4.3]$$

where P is the number of real particles, V_{1cell} is the volume of a cell and $N_{particles\ per\ cell}$ is the number of particles per cell. For the verification procedure, 9 simulations were performed, involving the variation of parameters such as the number of iterations, spatial discretization, time step, and number of molecules per cell. Table 1 presents the information regarding the parameters and their variations in the analyzed cases. In the table, λ represents the mean free path between molecules, and Δtres is the ratio between the cell dimension and the average velocity of the molecules.

Table 1. Parameters and their variations in simulated cases.

Cases	$N_{iteration}$	ΔX_{DSMC}	Δt_{DSMC}	$N_{molec.}$/cell
Case 1	100.000	λ/3	Δtres /5	20
Case 2	500.000	λ/3	Δtres /5	20
Case 3	1.000.000	λ/3	Δtres /5	20
Case 4	500.000	λ/3	2.Δtres /5	20
Case 5	500.000	λ/3	Δtres /10	20
Case 6	500.000	λ/3	Δtres /5	10

Case 7	500.000	λ/3	Δtres /5	40
Case 8	500.000	2λ/3	Δtres /5	20
Case 9	500.000	λ/6	Δtres /5	20

Cases 1, 2, and 3 were compared to evaluate the appropriate number of iterations to achieve low statistical noise. For spatial discretization evaluation, cases 2, 8, and 9 were compared. For Δtres, the comparison was made between cases 2, 4, and 5. Finally, in evaluating the impact of the number of molecules per cell, cases 2, 6, and 7 were compared. For all comparisons, the magnitude of centerline velocity and the pressure distribution along the microchannel were analyzed. Due to the large amount of results analyzed in the verification step, only the evaluation spatial discretization will be presented as a figure. This comparison can be observed in Figure 3.

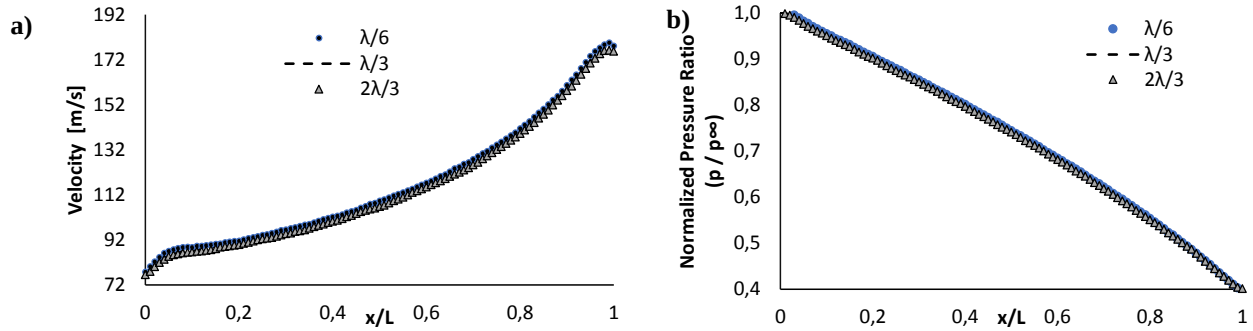

Figure 3. a) Comparison of cases 2, 8, and 9 in terms of the magnitude of velocity along the microchannel centerline. b) Comparison of cases 2, 8, and 9 in terms of the pressure along the microchannel centerline.

The results for the numerical verification of the DSMC simulations are presented in Table 2 where the relative difference of the analyzed parameters are shown.

Table 2. Relative difference of the parameters evaluated in verification step.

	In relation to Δtres /10		**In relation to 40 particles/cell**		**In relation to 1.000.000 Iterations**		**In relation to λ/6**	
	2Δtres /5	Δtres /5	10	20	100.000	500.000	2λ/3	λ/3
Normalized Pressure Ratio	0,85%	0,15%	0,71%	0,25%	-1,12%	0,01%	0,41%	0,42%
Velocity Magnitude	-3,53%	-1,29 %	-2,11%	0,27%	-4,37%	0,007%	-3,21%	0,86%

It is observed that the intermediate configurations represent the best compromise in terms of a computational cost. Thus, the verification of the dsmcFoamPlus implementation ensures the adequacy of the presented parameters: simulation time of 500,000 iterations, spatial discretization equal to one-third of the mean free path of the undisturbed flow, temporal discretization equal to one-fifth of the residence time, and an equivalent number of particles corresponding to approximately 20 DSMC molecules per cell.

Next, for the validation procedure, Case 2 was used, in which the parameters were adjusted as given by the verification results. The validation was performed by comparing the centerline channel pressure obtained in the simulations with the analytical solution and with the results obtained by Liou and Fang, (2001); White,(2013) and Roohi et al.,(2009).

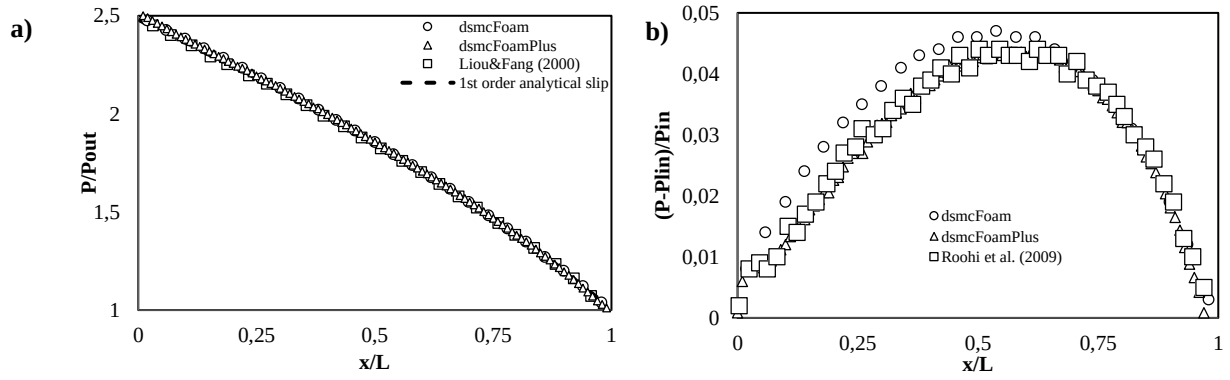

Figure 4. a) Comparison between the dsmcFoamPlus simulation, Liou and Fang, (2001) and White,(2013), and the analytical solution of pressure distribution along the centerline of a microchannel. b) Comparison between the dsmcFoamPlus simulation, White,(2013) and Roohi et al.,(2009) of the variation of a conventional linear pressure profile.

The DSMCFoamPlus results show good agreement with those obtained by Liou and Fang, (2001); White,(2013) and Roohi et al.,(2009). The observed variations arise from differences in some simulation parameters, such as the number of molecules used in each simulation, spatial discretization, and time step. The results also compare well to the numerical data presented by Roohi et al.(2009). With the verification and validation steps completed, the evaluation of flow properties in different microchannel geometries was carried out.

4.2 **Cases analyzed**

The simulations presented in this work investigated the rarefied subsonic flow through different microchannel geometries with a constant pressure ratio of 3. The simulations were conducted under isothermal conditions at 300K. The DSMC simulations were performed for Knudsen numbers of 0.027, 0.055, and 0.11 along straight microchannels, a 90-degree bend, and a rounded 90-degree bend. The results were compared to those of an equivalent straight microchannel geometry.

The input parameters such as the number of iterations, time step, and number of molecules per cell were chosen based on the results obtained from the verification and validation procedures. All geometries have the same aspect ratio (*AR*) of 10 with a microchannel height of 1μm by a length of 10μm with the flow properties always measured along the centerline of the geometries. In the 3 selected geometries, the meshes assigned for the entire domain are square cells with a dimension of λ/3, that is, for each Knudsen number defined there is a λ value and thus a corresponding mesh assigned. This value was defined due to the good compromise between computational cost and accuracy of the results obtained in the verification stage. On the wall, diffusive boundary conditions were applied and for the entrance and exit of the microchannels, the boundary conditions (mentioned in the Methodology section) of Fang & Liou (2002) and Wang & Li, (2004) were applied, respectively.

5. RESULTS

The data resulting from the DSMC simulations performed in the OpenFOAM software were extracted using the post-processing capabilities of the Paraview software. To provide a clear and organized presentation of the results for better understanding, the outcomes will be presented in distinct sections: Profile velocity outlet, Properties along the Microchannels and Mass Flow Analysis. This division allows for a comprehensive examination of the results and the overall analysis of the geometry variation on the flow properties.

5.1 **Profile velocity at the outlet**

In order to obtain the velocity magnitude and velocity profile for different Knudsen numbers, the outlet section of the straight microchannel was chosen for this analysis, and the results are presented in Figure 5.

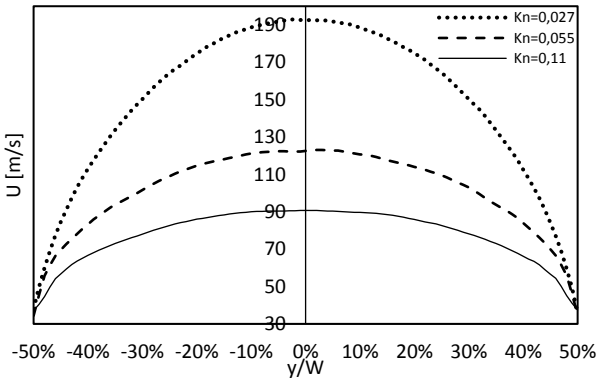

Figure 5. Velocity profile at the outlet of a straight microchannel for different Knudsen numbers.

For all cases, the velocity distribution shows a maximum value at the middle point of the microchannel and slip flow behavior on the channel walls. This behavior is consistent with what is observed for two-dimensional Poiseuille flow simulations. In Figure 5, a parabolic velocity profile can be observed at the microchannel outlet. Microchannels with lower Knudsen numbers exhibit higher velocity magnitudes.

5.2 **Properties along the Microchannels**

Figure 6 presents the distribution of the Knudsen number (a), Mach number (b), and Pressure (c) along the microchannel with a curved geometry and a Knudsen number of 0.027. For the other studied configurations, the magnitude and distribution of pressure and Mach number are shown in Figures 8 and 9.

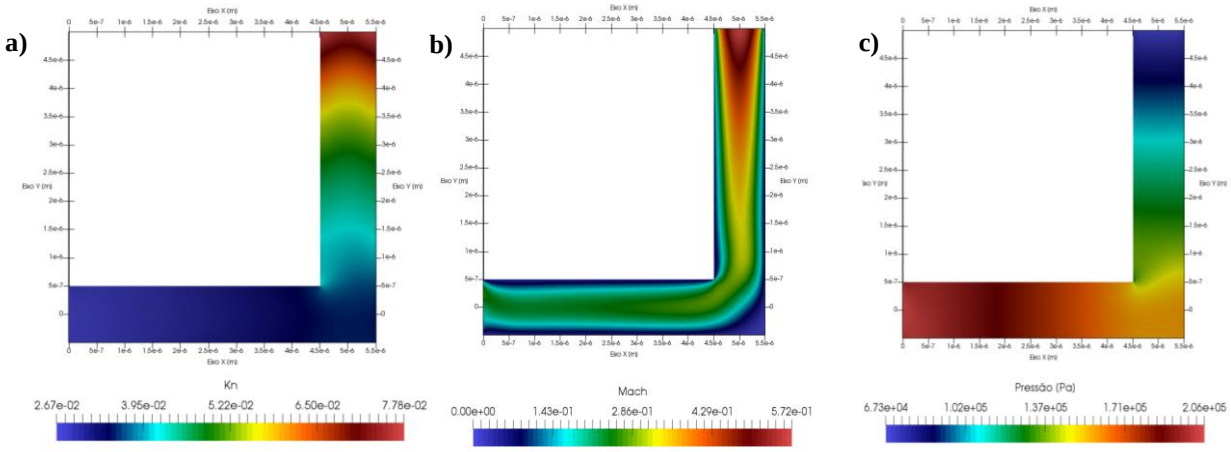

Figure 6. Distribution of the Knudsen number (a), Mach number (b), and Pressure (c) along the microchannel with a curved geometry and a Knudsen number of 0.027.

Figure 7 shows the streamlines along the microchannel with curved geometry and a Knudsen number of 0.027. The streamlines near the curve, shown in Figure 7a, suggest that the flow smoothly follows along the curved microchannel. The corresponding vector plot is shown in Figure 7b, with contours depicting the magnitude of velocity normalized by the speed of sound in the latter figure. The aforementioned observations are consistent with low Reynolds number flows in macrochannels. The decrease in velocity along the central line near the curve, coupled with the larger available area for flow in the curve, is responsible for the sharp decrease in velocity in the flow direction along the central line in the curve, as seen in Figure 7a.

The slow flow at the corner of the curve results in a secondary motion (Figure 7b). However, the Reynolds number at which this recirculation motion appears is quite low compared to macroscopic flows, suggesting that the Knudsen number may play a significant role in determining the moment when the secondary flow sets in.

The experiments by Li et al. (2000) and Lee et al. (2001) indicate that recirculation indeed appears at low Reynolds numbers in complex microchannels, which is consistent with the current simulations. Note that in Figure 7b, the recirculation motion has a size larger than that of a cell (approximately the size of 4 cells). Although this size helps to rule out the possibility of this phenomenon appearing due to statistical noise, its size makes it difficult to detect in experiments. The appearance of recirculation at low Reynolds numbers is surprising since it was initially thought that, due to the slip condition at the wall, velocity gradients would be reduced, leading to a decrease in vorticity generation and a corresponding delay in the formation of recirculation motion. These vortices were already observed by White (2013) using de DsmcFoamPlus, but with different simulation parameters.

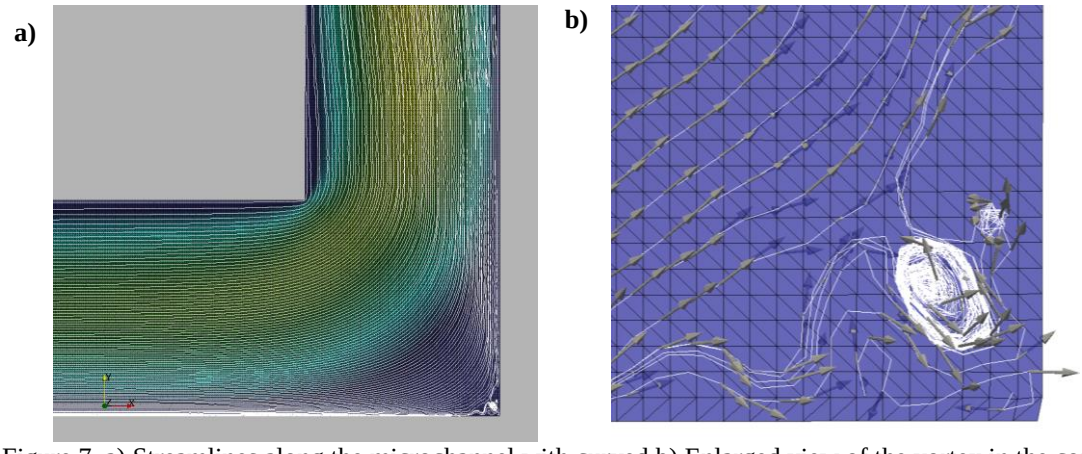

Figure 7. a) Streamlines along the microchannel with curved b) Enlarged view of the vortex in the corner.

The distributions of normalized pressure along the centerline for the nine cases are shown in Figure 8, presenting the three different geometries for the Knudsen numbers: a) 0.027, b) 0.055, and c) 0.11. As expected, nonlinear pressure profiles were found, and the degree of nonlinearity decreases with increasing Knudsen number as rarefaction effects (Kn) begin to dominate over compressibility effects (Ma).

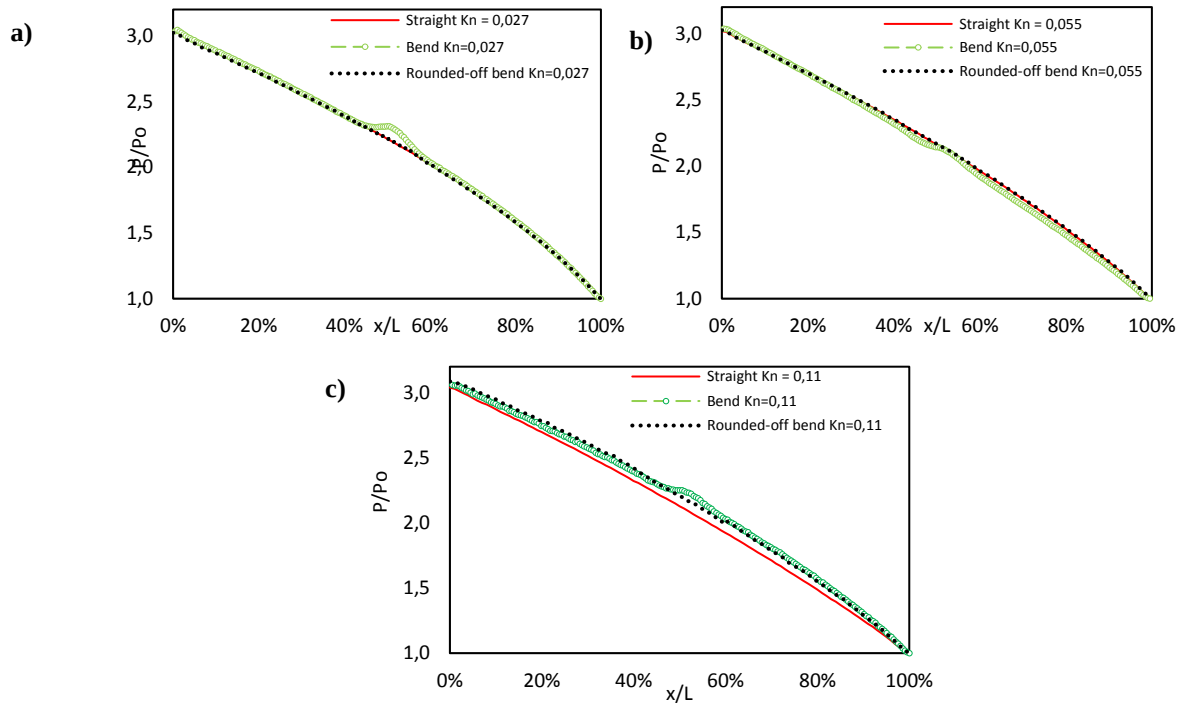

Figure 8. Normalized pressure ration for the following Knudsen a) 0,027 b) 0,055 e c) 0,11.

In Figure 9, the distributions of the Mach number along the microchannel were obtained, and a similar behavior to the pressure profile was observed. A higher degree of rarefaction exhibited greater linearity compared to the simulation with a lower Knudsen number. To present the distribution of the Mach number along the microchannel, Figure 9 shows, in each graph, the three Knudsen numbers studied and the three geometries: a) Straight, b) Bend, and c) Rounded-off bend.

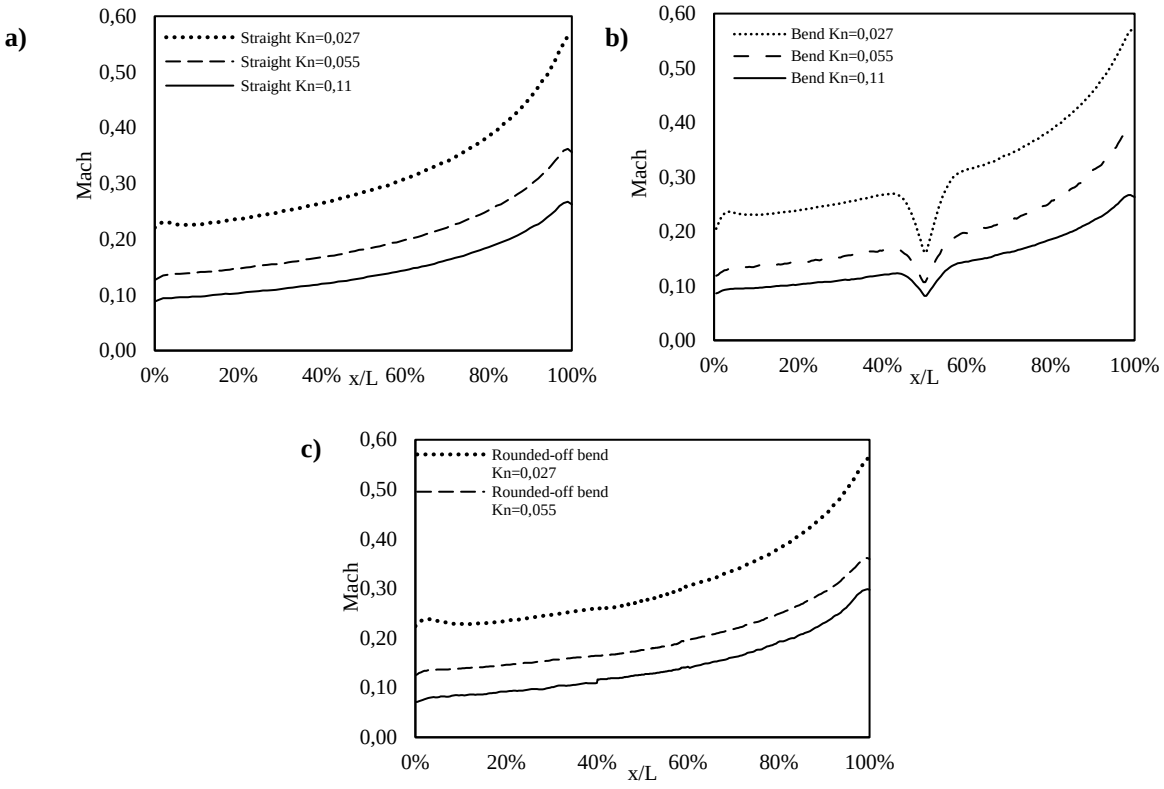

Figure 9. Mach number distribution for the following geometries a) straight b) microchannel with bend e c) microchannel with rounded-off bend.

5.3 **Mass Flow Analysis**

Figure 10 shows the behavior of mass flow rate for the different analyzed geometries and Knudsen numbers. It can be observed that the magnitude of mass flow rate decreases with increasing Knudsen number, and it allows for comparing the variations of mass flow rate with respect to a straight microchannel, considering the degree of rarefaction that the flow is subjected to.

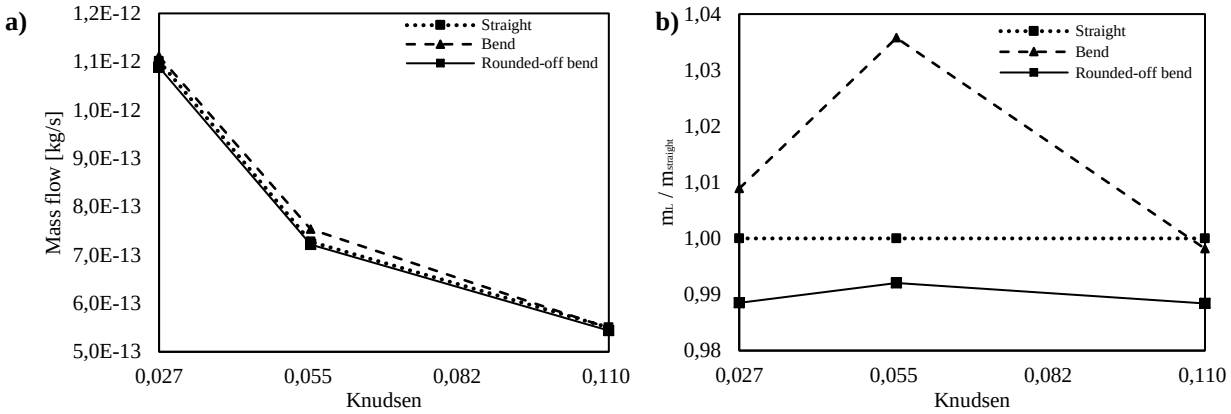

Figure 10. a) Mass flow for different geometries and Knudsen numbers. b) Normalized mass flow by straight microchannel for different geometries and Knudsen numbers.

The velocity and pressure distributions suggest that the mass carrying capacity, for a given pressure ratio, is practically the same for both straight and curved microchannels. Figure 10b shows that the ratio of mass flow rate for the curved microchannel, mL, to the mass flow rate for the straight microchannel, mstraight, remains close to unity for the range of investigated Knudsen numbers. In fact, for Kn > 0.055, the mL/mstraight ratio decreases, while for Kn < 0.055, the mL/mstraight ratio increases from the denser cases up to approximately Kn = 0.055. In other words, a curved microchannel can transport between 1% to 3% more mass than the corresponding straight microchannel for Knudsen numbers smaller than 0.055. For Knudsen numbers close to 0.1, both the results using DSMC and the study conducted by Agrawal et al. (2009), which employed the Lattice Boltzmann method, exhibited ratios of mass flux between a curved microchannel and a straight microchannel that were approximately unity. However, for Knudsen numbers below 0.1, Agrawal et al. (2009) discovered higher mass flux values for a straight microchannel compared to a curved one. Conversely, our findings in this study revealed the opposite behavior for the same Knudsen numbers, indicating that more investigations need to be performed to clarify these results..

6. CONCLUSION

DSMC simulations were performed for gas flow through microchannels with different geometries, covering Knudsen numbers between 0.027 and 0.11. The behavior of pressure and velocity away from the bend is similar to that of a straight microchannel. The velocity continuously increases with the streamwise coordinate and with an increase in the Knudsen number. The presence of a secondary flow is observed near the bend only for the case with a curved geometry and a Knudsen number of 0.027, indicating that the Knudsen number may play an important role in the onset of recirculation.

The pressure profiles in the cases with a bend differ from those of the straight channel due to noticeable jumps in the local pressure at the location of the bend. These jumps are compressibility effects introduced by the reduction in gas velocity in the flow direction due to abrupt changes in the channel geometry.

It is observed that in the configurations with a bend, the evaluated parameters exhibit slightly higher magnitudes in the rounded configuration compared to the sharp corner configuration, a behavior typically observed for low Knudsen numbers where the tends to the continuum.

The distribution of Mach number and pressure between the curved microchannel and the straight microchannel is similar, and the similarity increases when a rounding is added to the bend configuration. This indicates that the flow is not aware of the presence of the bend. This result is explained based on the rarefaction of the gas. It is also observed that the mass flow rate through a rounded-off microchannel can be slightly higher than that of a straight microchannel with the same length, pressure ratio, and the same amount of gas flowing through them. However, this result needs further validation. It must be pointed out that, for the case of micro and nanoflows numerical studies play an important role due to the scarcity of detailed experimental data in the literature.

Most notably, it was found that adding curvature to the bend can eventually lead to an increase in the mass flow rate through the channel, even in cases where, under the same boundary conditions, adding a sharp bend would result in a decrease in the mass flow rate. This is an important finding that can be valuable in practical applications.

7. ACKNOWLEDGEMENTS

This study was financed in part by the Coordenação de Aperfeiçoamento de Pessoal de Nível Superior – Brasil (CAPES) – Finance Code 0001.

Research carried out using the computational resources of the Center for Mathematical Sciences Applied to Industry (CeMEAI) funded by FAPESP (grant 2013/07375-0).

8. REFERENCES

AGRAWAL A., DJENIDI L., AGRAWAL A., Simulation of gas flow in microchannels with a single 90° bend. **Computers & Fluids 38** 2009; 1629–1637.

BIRD, G., **Molecular Gas Dynamics and the Direct Simulation of Gas Flows**, Clarendon, Oxford, 1994.

CERCIGNANI, C., **Rarefied gas dynamics: from basic concepts to actual calculations**, Cambridge University Press, 2000.

FANG, Y.; LIOU, W. W. Computations of the flow and heat transfer in microdevices using dsmc with implicit boundary conditions. **J. Heat Transfer**, v. 124, n. 2, p. 338–345, 2002.

GAD-EL-HAK M. The fluid mechanics of microdevices. **Journal of Fluids Engineering**; pp. 121:5–33, 1999.

LE M., HASSAN I.,ESMAIL N., The effects of outlet boundary conditions on simulating supersonic microchannel flows using DSMC, **Appl. Therm. Eng**. 27 (2007) 21-30

LEE S.Y.K, WONG M., ZOHAR Y. Gas flow in microchannels with bends. **J MicromechMicroeng** 2001;11:635–44.

LI X., LEE W.Y., WONG M., ZOHAR Y. Gas flow in constriction microdevices. **SensActuat A** 2000;83:277–83.

LIOU W.W., FANG Y., Heat transfer in microchannel devices using DSMC, **J. Microelectromech. Syst**. 10 (2001) 274-279.

NANCE, R. P.; HASH, D. B.; HASSAN, H. Role of boundary conditions in monte carlo simulation of microelectromechanical systems. **Journal of Thermophysics and Heat Transfer**, v. 12, n. 3, p. 447–449, 1998.

OpenFOAM Foundation, "http://www.openfoam.org/," 2019.

ROOHI E., DARBANDI M., and MIRJALILI V. Direct simulation Monte Carlo solution of subsonic flow through micro/nanoscale channels. **Journal of Heat Transfer**, 131(9):092402, 2009.

SCANLON, T. J., ROOHI, E., WHITE, C., DARBANDI, M., and REESE, J. M., **An Open Source, Parallel, DSMC Code for Rarefied Gas Flows in Arbitrary Geometries**, Computers & Fluids, Vol. 39, 2010, pp. 2078–2089.

SEBASTIÃO I. B., SANTOS W.F.N., Gas-surface interaction effects on the flowfield structure of a high speed microchannel flow, **Applied Thermal Engineering** 52 (2013) 566-575

SEBASTIÃO I. B., SANTOS W.F.N., Gas-surface interaction impact on heat transfer and pressure distributions of a high speed microchannel flow, **Applied Thermal Engineering** 62 (2014) 58-68

SHARP K.V., ADRIAN R.J., SANTIAGO J.G., MOLHO J.I. **Liquid flows in microchannels**. In: Gad-el-Hak M, editor. The MEMS handbook. Boca Raton: CRC Press; 2002.

WANG, M.; LI, Z. Simulations for gas flows in microgeometries using the direct simulation monte carlo method. **International Journal of Heat and Fluid Flow**, Elsevier, v. 25, n. 6, p. 975–985, 2004.

WHITE C., **Bechmarking, development and applications of an open source DSMC solver**, Ph.D, thesis, University of Strathclyde, Glasgow, Scotland (2013).

XIE J., BORG M. K., GIBELLI L., HENRICH O., LOCKERBY D. A., REESE J. M. Effective mean free path and viscosity of confined gases. **Physics of Fluids** 31, 072002 (2019).

9. RESPONSIBILITY NOTICE

The authors are the only responsible for the printed material included in this paper.